

Role of *luxS* in *Bacillus anthracis* growth and virulence factor expression

Marcus B. Jones,^{1,3,*} Scott N. Peterson,¹ Rosslyn Benn,¹ John C. Braisted,¹ Behnam Jarrahi,¹ Kenneth Shatzkes,¹ Dacheng Ren,⁴ Thomas K. Wood⁵ and Martin J. Blaser^{2,3}

¹Pathogen Functional Genomics Resource Center (PFGRC); J. Craig Venter Institute (JCVI); Rockville, MD USA; ²Department of Medicine; New York University School of Medicine; New York, NY USA; ³Department of Microbiology; Sackler Institute; New York University School of Medicine; New York, NY USA; ⁴Departments of Biomedical and Chemical Engineering; Civil and Environmental Engineering; and Biology; Syracuse Biomaterials Institute; Syracuse University; NY, USA; ⁵Artie McFerrin Department of Chemical Engineering; Texas A&M University; College Station, TX USA

Keywords: *luxS*, virulence, quorum-sensing, microarray, furanone

Quorum-sensing (QS), the regulation of bacterial gene expression in response to changes in cell density, involves pathways that synthesize signaling molecules (auto-inducers). The *luxS/AI-2*-mediated QS system has been identified in both Gram-positive and Gram-negative bacteria. *Bacillus anthracis*, the etiological agent of anthrax, possesses genes involved in *luxS/AI-2*-mediated QS, and deletion of *luxS* in *B. anthracis* Sterne strain 34F₂ results in inhibition of AI-2 synthesis and a growth defect. In the present study, we created a $\Delta luxS$ *B. anthracis* strain complemented in trans by insertion of a cassette, including *luxS* and a gene encoding erythromycin resistance, into the truncated *plcR* regulator locus. The complemented $\Delta luxS$ strain has restored AI-2 synthesis and wild-type growth. A *B. anthracis* microarray study revealed consistent differential gene expression between the wild-type and $\Delta luxS$ strain, including downregulation of the *B. anthracis* S-layer protein gene EAI and pXOI virulence genes. These data indicate that *B. anthracis* may use *luxS/AI-2*-mediated QS to regulate growth, density-dependent gene expression and virulence factor expression.

Introduction

Bacillus anthracis is a gram-positive, non-motile, rod-shaped bacterium that is the etiological agent of anthrax.¹⁻³ The virulent nature of *B. anthracis* is attributed to two large plasmids, the 181.6 kb pXO1 and the 96.2 kb pXO2, that encode primary pathogenetic factors, including toxin production and capsule formation, respectively.⁴⁻¹² The three proteins that comprise the two *B. anthracis* toxins are lethal factor (LF), edema factor (EF) and protective antigen (PA). In two different combinations, these three proteins comprise the lethal toxin (PA + LF) and the edema toxin (PA + EF).^{5,7,9-18} Maximum production of toxins occurs during the transition from log to the stationary phase of growth, suggesting growth phase-regulation of expression.¹⁹

Quorum-sensing (QS) is a process by which bacteria regulate the expression of density- and growth phase-dependent genes.²⁰⁻²⁵ QS involves the synthesis, release and detection of small signaling molecules, termed auto-inducers. The auto-inducer concentration is directly correlated to the bacterial population. Utilization of QS systems is critical for the regulation of virulence gene expression in many pathogenic bacteria. Inhibition of QS circuits by QS antagonists, such as the halogenated furanones from the red-sea alga *Delisea pulchra*, offers an attractive method for inhibiting bacterial pathogens.²⁶⁻³⁶

B. anthracis synthesizes AI-2 or an AI-2-like auto-inducer molecule that induces bioluminescence in the *Vibrio harveyi*

bioassay.³⁷ Furthermore, analysis of the *B. anthracis* genome indicated the presence of a gene, *luxS*, which typically is involved in QS. Disruption of *luxS* resulted in the inability of *B. anthracis* to synthesize a functional AI-2 or AI-2-like molecule recognizable in the *V. harveyi* bioassay, and in a defect in growth in vitro for the *B. anthracis luxS* mutant.³⁷ These data suggest that *B. anthracis* may utilize the *luxS/AI-2* QS system to regulate growth as well as density-dependent gene expression.

In the present report, we characterize the differential gene expression of *Bacillus anthracis* strains 34F₂, 34F₂ $\Delta luxS$ and 34F₂*luxS*:comp. To further characterize the role of QS in *B. anthracis*, by microarray analysis we analyzed *B. anthracis* gene expression in wild-type cells grown in the presence or absence of halogenated furanones. Finally we utilize a custom tiled genome Affymetrix array to identify possible small RNAs differentially expressed in the *luxS* mutant compared to the wildtype.

Results

Complementation of AI-2 deficiency. Cell-free medium (CFM) was collected from *B. anthracis* strains 34F₂, 34F₂ $\Delta luxS$ and 34F₂*luxS*:comp for assessment in the *Vibrio harveyi* BB170 bioluminescence assay. The AI-2 bioassay utilizes a deficiency in the AI-1 sensor in *V. harveyi* strain BB170. Without the *luxN* AI-1 encoded sensor, strain BB170 only exhibits bioluminescence in response to AI-2 or an AI-2-like molecule. Growth of strain

*Correspondence to: Marcus B. Jones; Email: mjones@jcv.org

Submitted: 09/21/09; Revised: 11/24/09; Accepted: 11/30/09

Previously published online: www.landesbioscience.com/journals/virulence/article/10752

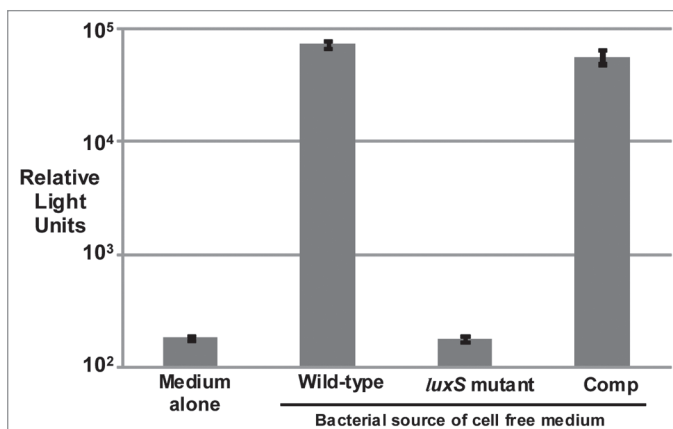


Figure 1. Induction of bioluminescence in *V. harveyi* reporter strain by CFM from *B. anthracis* cells. *V. harveyi* strain BB170 only upregulates the expression of the *lux* operon [measured as relative light units (RLU)], when AI-2 or AI-2-like molecules are present in its milieu. Cell free medium (CFM) obtained from AI-2-synthesizing bacteria can induce expression of the bioluminescence-generating *luxCDABE* operon in BB170. (A) In the experiments shown, CFM from 5-h cultures of *B. anthracis* strains 34F₂ and 34F₂ Δ *luxS* and sterile CFM alone were used as positive and negative controls. The baseline is the value when uninoculated (sterile) CFM alone at 5 h were used. Each bar represents the mean (\pm SD) of triplicate experiments. Compared to the negative and positive controls, 34F₂ Δ *luxS:comp* showed restored AI-2 activity compared to wild-type 34F₂. (B) In the experiment shown, CFM from 5-h cultures of wild-type 34F₂ and 34F₂ Δ *luxS:comp* were serially diluted 1:1, 1:10 and 1:100. Each bar represents the mean (\pm SD) of triplicate experiments.

BB170 overnight, followed by dilution 1:10,000 (to yield low cell density), reduces the level of endogenous AI-2 below the threshold required for luminescence. In this experimental system, the addition of exogenous AI-2 from bacteria possessing *luxS* function can restore the bioluminescence phenotype of the BB170 cells. As a negative control, the *V. harveyi* reporter strain BB170 was incubated with sterile cell-free medium (CFM) alone, and as a positive control, CFM from a high-density culture of strain BB170 was used (Fig. 1). Addition of sterile CFM to cells of BB170 served as the standard for baseline luminescence, whereas, as expected, addition of CFM from the high-density BB170 culture induced a >100-fold increase in luminescence. Additional controls included were CFM from *B. anthracis* strain 34F₂ Δ *luxS* (negative control) and *B. anthracis* 34F₂ (positive control). CFM from *B. anthracis* strain 34F₂ Δ *luxS:comp* exhibits AI-2 activity comparable to that of the wild-type strain (Fig. 1). These data demonstrate that the *luxS* chromosomal complementation fully restored AI-2 production that was deficient in *B. anthracis* strain 34F₂ Δ *luxS* (Fig. 1).

Complementation of the growth defect in *B. anthracis* strain 34F₂ Δ *luxS*. When cultured in liquid medium, *B. anthracis* 34F₂ Δ *luxS* exhibited a moderate, but reproducible, growth defect compared to wild-type *B. anthracis* 34F₂.³⁷ To determine whether the growth defect was directly related to the deletion of *luxS*, we compared the growth of *B. anthracis* wild-type strain 34F₂, strain 34F₂ Δ *luxS*, and the 34F₂ Δ *luxS:comp* strain. As determined by triplicate cell densities and based on OD₆₀₀, the 34F₂ Δ *luxS:comp* strain showed restored growth compared to the

Δ *luxS* strain (Fig. 2). These data suggest that *luxS*/AI-2-mediated quorum sensing is involved in regulating metabolic functions in *B. anthracis* under aerobic conditions. Based on these findings, we sought to characterize the growth defect in 34F₂ Δ *luxS* by examining the transcriptional profile of the 34F₂ Δ *luxS* strain compared to the wild type parental strain.³⁷

Differential gene expression of a *B. anthracis* 34F₂ Δ *luxS* strain grown aerobically. To identify genes regulated by the *luxS*/AI-2 QS system, *B. anthracis* microarrays were utilized. Total RNA was isolated from *B. anthracis* strains 34F₂ and 34F₂ Δ *luxS* grown in BHI in the absence of sodium bicarbonate. Isolated RNA samples were hybridized to spotted *B. anthracis* array slides and analyzed using TM4 software (www.tm4.org).³⁸ Significance of microarray (SAM) analysis of array data revealed that 576 genes were differentially expressed in the 34F₂ Δ *luxS* strain, compared to the wild-type 34F₂ strain based on a false discovery cutoff of 7%. Select upregulated genes \geq 2-fold (Table 2) and downregulated genes \geq 2-fold (Table 3) are listed. Genes that were not downregulated \geq 2-fold, but are in the middle of a presumed operon in which other genes have a \geq 2-fold change are included. Among the genes downregulated in the 34F₂ Δ *luxS* strain are the *luxS* gene (as expected), the S-layer virulence gene EA1, encoding putative S-layer proteins, and genes involved in phosphotransferase systems (PTS) (Table 3). Genes that were upregulated \geq 2-fold included those encoding a phospholipase C, a bacitracin protease and resistance protein (Table 2). These data suggest that *luxS*/AI-2 is involved in regulating peptide transport and S-layer expression. To further elucidate impact of *luxS*/AI-2 on *B. anthracis* gene expression we performed an analysis of down and upregulated genes to determine cellular and functional roles. Analysis of downregulated genes revealed that a significant portion are involved in energy metabolism (23%) and transport and binding proteins (12.7%), and analysis of upregulated genes revealed a significant portion are involved with cellular processes (18.8%).

Closer examination of genes downregulated in *B. anthracis* 34F₂ Δ *luxS* strain revealed several operons involved in nitrate/nitrite metabolism (Table 3) when grown either aerobically or in the presence of sodium bicarbonate. Nitrate reduction has three fundamental roles: (1) utilization as a nitrogen source (nitrate assimilation); (2) maintenance of oxidation-reduction balance (nitrate dissimilation), and (3) utilization as a terminal electron acceptor (nitrate respiration).³⁹ In-depth analysis of nitrate/nitrite respiration regulation in *B. subtilis* revealed the ability of the bacterium to convert nitrate or nitrite to ammonium when grown aerobically.⁴⁰ The conversion of these nitrogen sources to ammonium is catalyzed by assimilatory nitrate and nitrate reductases. Mutation in *nasD*, *nasE* or *nasF* (assimilatory nitrite reductases) led to growth defects in *B. subtilis* when glucose was depleted.⁴⁰ These observations coupled with the transcriptional profile of the 34F₂ Δ *luxS* strain, suggests that *luxS*/AI-2 may play a role in regulating nitrate/nitrite metabolism in *B. anthracis*, and that the observed growth defect in the *luxS* mutant is due to the inability to utilize nitrate/nitrite. It is interesting to note that complementation of *luxS* in *B. anthracis* strain 34F₂ Δ *luxS* did not fully restore the transcriptional expression of the nitrate/nitrite regulon to wildtype

levels

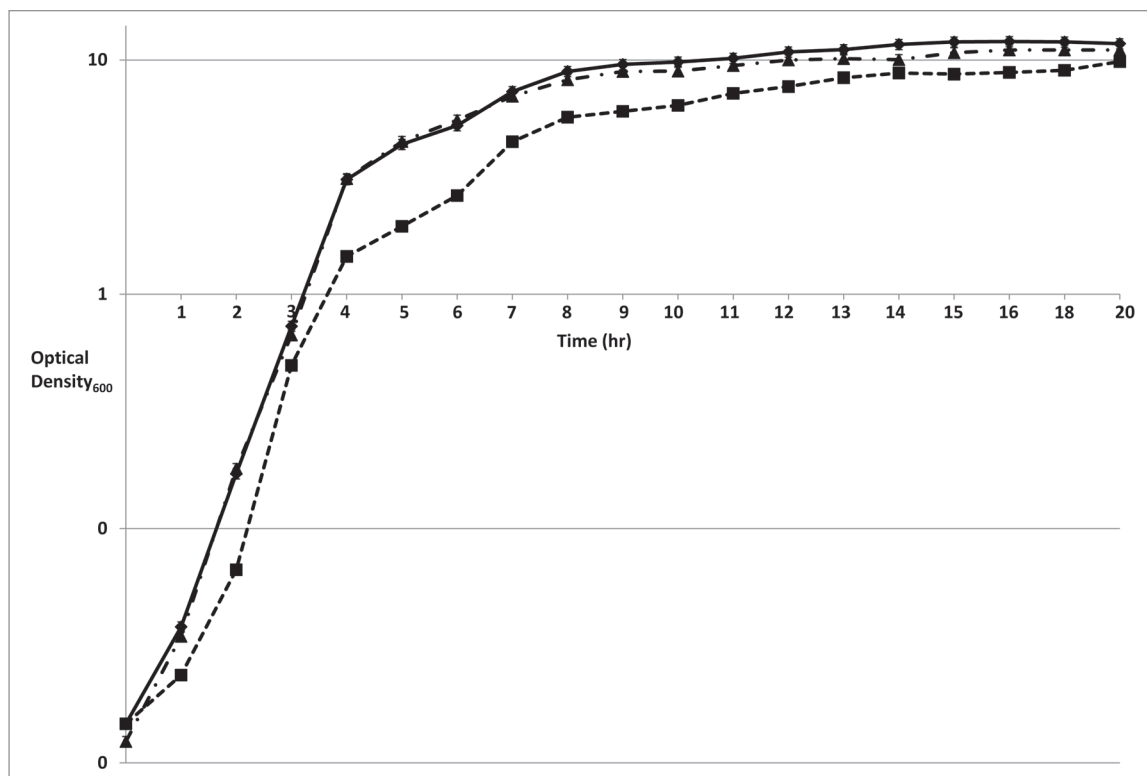


Figure 2. Growth rate analysis of *B. anthracis* 34F₂ΔluxS:comp. *B. anthracis* strains 34F₂, 34F₂ΔluxS, and 34F₂ΔluxS:comp were grown overnight and diluted in sterile BHI media to an optical density (OD₆₀₀) of ≈0.01. Cell growth was monitored, CFM removed and passed through a 0.2 μm filter for use in the *V. harvey* bioassay. The graph represents the mean (±SD) of triplicate experiments performed on the same day. Solid line with filled diamonds represent strain 34F₂, dotted line with filled squares represent strain 34F₂ΔluxS and short dash line with filled triangles represents strain 34F₂ΔluxS:comp.

(data not shown), suggesting that additional factors may contribute to the growth defect of the *luxS* mutant, and that *luxS*/AI-2 quorum-sensing is not the only factor regulating nitrate/nitrite metabolism. To further elucidate the potential role of *luxS*/AI-2 in nitrate/nitrite metabolism we will make use of inhibitors of AI-2-mediated quorum-sensing.

Differential gene expression of *B. anthracis* 34F₂ΔluxS grown with 0.8% sodium bicarbonate. QS has been implicated in the regulation of virulence gene expression for a number of pathogenic bacteria.^{24,28,30,41-48} To identify genes regulated by the *luxS*/AI-2 QS system and CO₂/bicarbonate, total RNA was isolated from *B. anthracis* strains 34F₂ and 34F₂ΔluxS grown in BHI in the presence of 0.8% sodium bicarbonate. CO₂/bicarbonate is critical for activation of toxin gene expression in *B. anthracis*. Isolated RNA samples were hybridized to spotted *B. anthracis* array slides and analyzed using Spotfinder and TMeV software. Analysis of the microarray data revealed substantial differential expression of virulence genes on plasmid pXO1 in the 34F₂ΔluxS strain compared to the parental strain 34F₂. Genes downregulated on pXO1 include the protective antigen (*pagA*), *pagR*, lethal factor (*lef*) and the calmodulin-sensitive adenylate cyclase (*cya*) (Table 4, Fig. 3). Figure 3 demonstrates temporal changes in gene expression within the pathogenicity island on pXO1 in strain 34F₂ΔluxS with regard to the downregulation of the toxin components. The virulence regulator *atxA* was only

slightly downregulated in the 34F₂ΔluxS strain compared to the wild type, suggesting that *luxS*/AI-2 influence on expression of the toxin components is regulated by factors in addition to *atxA*. Analysis of the transcriptional profile of the 34F₂ΔluxS complement strain revealed near wildtype levels of toxin components *pagA*, *lef* and *cya* compared to the *luxS* mutant strain (Table 5). Based on these data, we hypothesize that *luxS*/AI-2 may play a role in influencing additional regulators that modulate toxin expression.

Effect of halogenated furanones on *B. anthracis* gene expression. To better understand the mechanism by which *B. anthracis* may utilize *luxS*/AI-2-mediated QS to regulate gene expression, we studied the effect of halogenated furanones in microarray experiments. Previous studies showed that halogenated furanones can inhibit AI-2-regulated genes in *E. coli* without inhibiting bacterial growth. However, our recent data showed that halogenated furanones inhibit *B. anthracis* growth in a dose-dependent manner.³⁰ *B. anthracis* cultures were grown to mid-log phase and then supplemented with diluent alone (negative control) or diluent with 20 μg/ml of fur-2.³⁰ This concentration of fur-2 was selected due to its ability to inhibit expression of *B. anthracis* toxin gene promoter: *lacZ* fusions, and because fur-2 showed no significant toxicity to human THP-1 monocytes at concentrations ≤20 μg/ml (unpublished data). The data reveal that fur-2 can stimulate or inhibit *B. anthracis* gene expression

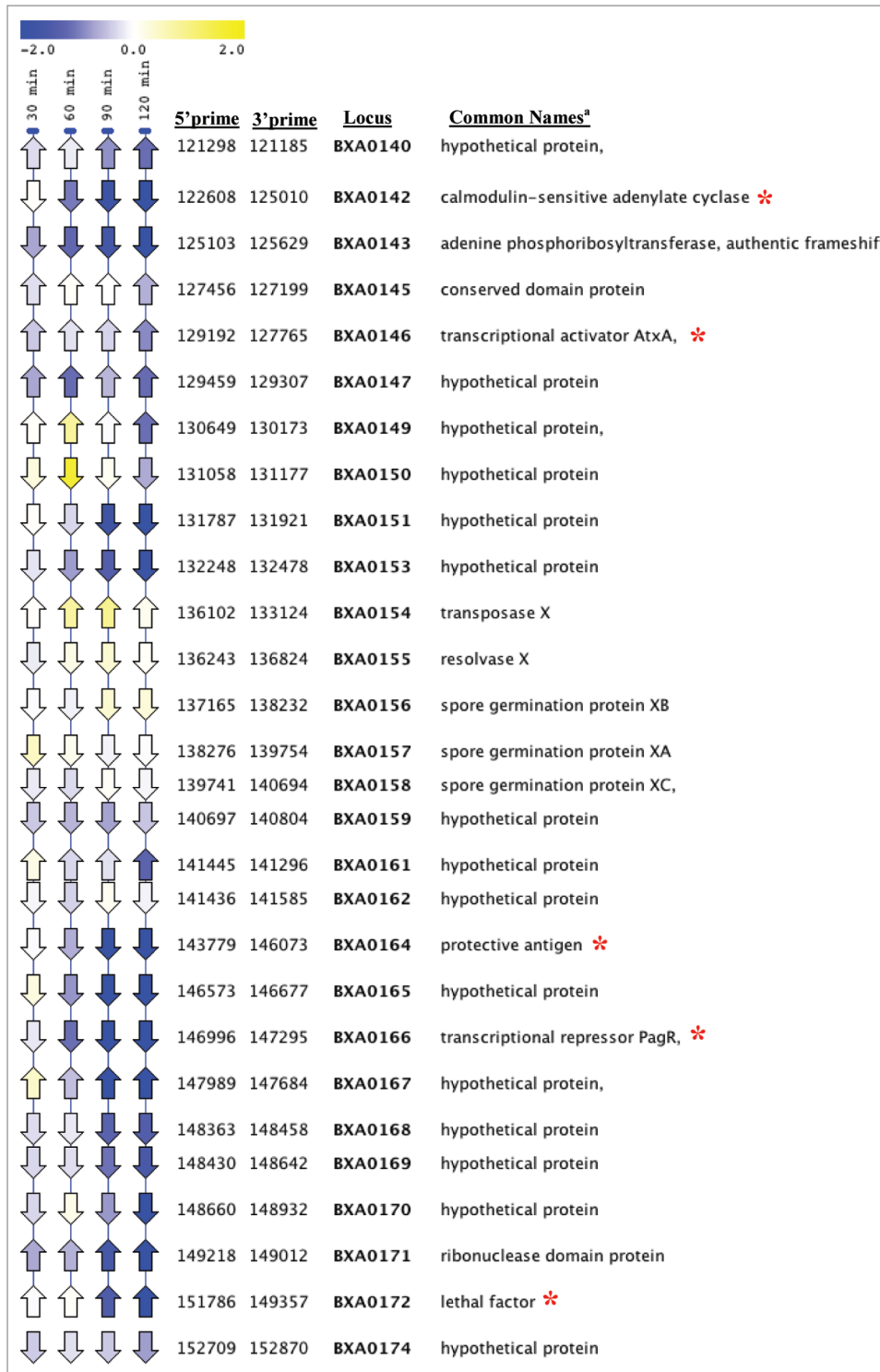


Figure 3. Analysis of pXOI pathogenicity island gene expression in *B. anthracis* strain 34F₂Δ*luxS* compared to strain 34F₂ using Linear Expression Map (LEM) viewer. Time points are indicated at the top of each column. Arrows indicate the direction of gene orientation. The color scale indicates the log₂ changes in expression, according to the scale shown above. Locus ID based on *B. anthracis* Florida strain A2012. ^aGenes bolded relate to production or regulation of toxins. ^bRed asterisk indicates virulence genes.

(Fig. 4). Inhibition and stimulation by *fur-2* was not a global event, with only ~5% of the genome showing ≥3-fold differential expression. Expression of the *B. anthracis* toxin components (*lef* and *pagA*) on pXOI were significantly downregulated two hours

post-exposure to *fur-2* (Table 6). These data are consistent with the observation that *fur-2* significantly inhibits expression of *lacZ* fusions to the promoters of the toxin components.³⁰ In addition to the toxin components, furanone treatment of *B. anthracis* cells

inhibited respiratory nitrate systems as mentioned above.

To determine whether *fur-2* was inhibiting genes regulated by the *luxS/AI-2* QS system, the differentially expressed genes in cells treated with *fur-2* were compared to those differentially expressed in the *B. anthracis* $\Delta luxS$ strain (Tables 2 and 3). Analysis of microarray data revealed that *B. anthracis* toxin components and respiratory nitrate reductase systems were downregulated under both experimental conditions (Fig. 4). However, *fur-2* did not inhibit the expression of *luxS* directly. These data indicate that *fur-2* does not directly inhibit the transcriptional activity of *luxS*, but may interact with the *luxS* product at the cellular level. Furthermore, *fur-2* inhibits genes that may be regulated by *luxS/AI-2* mediated QS in *B. anthracis*. These data support the hypothesis that *luxS/AI-2*-mediated QS may play a role in the regulation of the *B. anthracis* toxin components (*pagA*, *lef* and *cya*) and nitrate/nitrite metabolism.

Analysis of small RNAs in *B. anthracis* 34F₂ $\Delta luxS$ strain. Small RNAs have been implicated in regulating pathways involved in QS.⁴⁹ To investigate the effect of a *luxS* mutation on small RNAs in *B. anthracis*, we utilized an Affymetrix custom genome tiled array. This platform permitted us to investigate the transcriptional activity of small and antisense RNAs. Analysis of pXO1 revealed several regions on the virulence plasmid demonstrating differential transcriptional activity in intergenic regions (Fig. 5). The intergenic region between locus BXA0122 and BXA0124 had substantial transcriptional activity. Furthermore, a comparison of the 34F₂ $\Delta luxS$ strain with the wildtype demonstrated a lower transcriptional profile, suggesting that *luxS/AI-2* may play a role in regulating the transcriptional activity of small RNAs in *B. anthracis*. However, to better understand the regulatory network of *luxS/AI-2*-mediated QS, additional experiments will be necessary.

Discussion

In this study, we were able to complement the *luxS/AI-2* deficiency in the 34F₂ $\Delta luxS$ mutant. First, we assessed whether insertion of the *luxS* ORF plus its putative promoter into the *plcR* locus, creating 34F₂ $\Delta luxS$:comp strain, would restore *luxS/AI-2* activity. Cell-free medium collected from the 34F₂ $\Delta luxS$:comp strain was able to fully stimulate luminescence in the *V. harveyi* reporter strain (Fig. 1), indicating that the *B. anthracis* 34F₂ $\Delta luxS$:comp strain produces AI-2 or an AI-2-like molecule,

likely similar in structure to AI-2 from *V. harveyi*. Serial dilutions of CFM collected from the 34F₂ $\Delta luxS$:comp strain were able to stimulate luminescence in the *V. harveyi* strain to a similar extent as the wild-type 34F₂ strain, providing strong evidence that the strain is fully complemented for AI-2 activity. The growth defect observed in the *B. anthracis* $\Delta luxS$ strain suggests that *luxS* is involved in regulating *B. anthracis* growth. That the growth of *B. anthracis* strain $\Delta luxS$:comp was restored to wildtype levels (Fig. 2) provides direct evidence that *luxS* is in fact involved in regulating *B. anthracis* growth. Regulation of growth by *luxS*

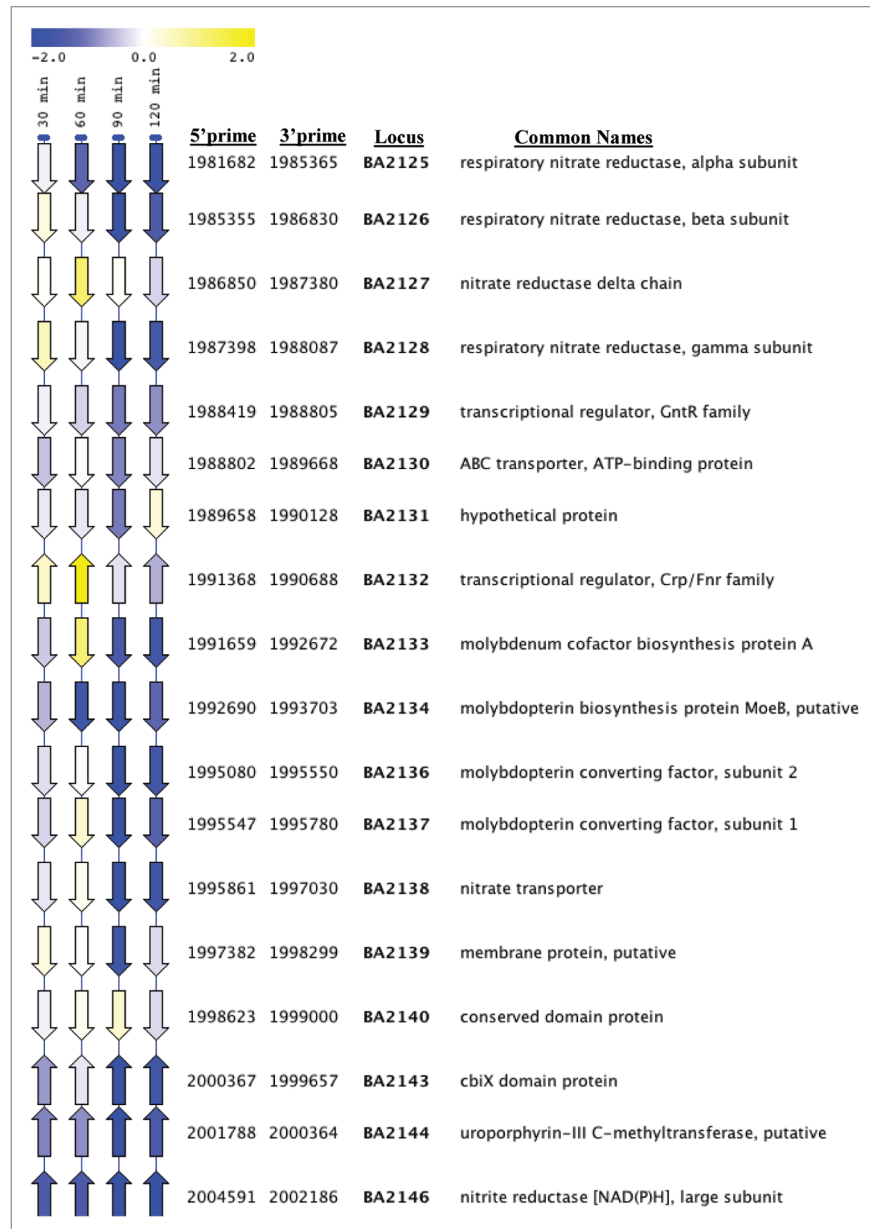


Figure 4. Analysis of respiratory nitrate genes in strain 34F₂ $\Delta luxS$ compared to strain 34F₂ and strain 34F₂ exposed to 20 μ g/ml of *fur-2* using LEM. Time points (left-most 4 columns) and sample (exposure to *fur-2* for one hour; right-most column) are indicated at the top of each column. Arrows indicate the direction of gene orientation. The color scale indicates the log₂ changes in expression, according to the scale shown above. Locus ID based on *B. anthracis* strain Ames.

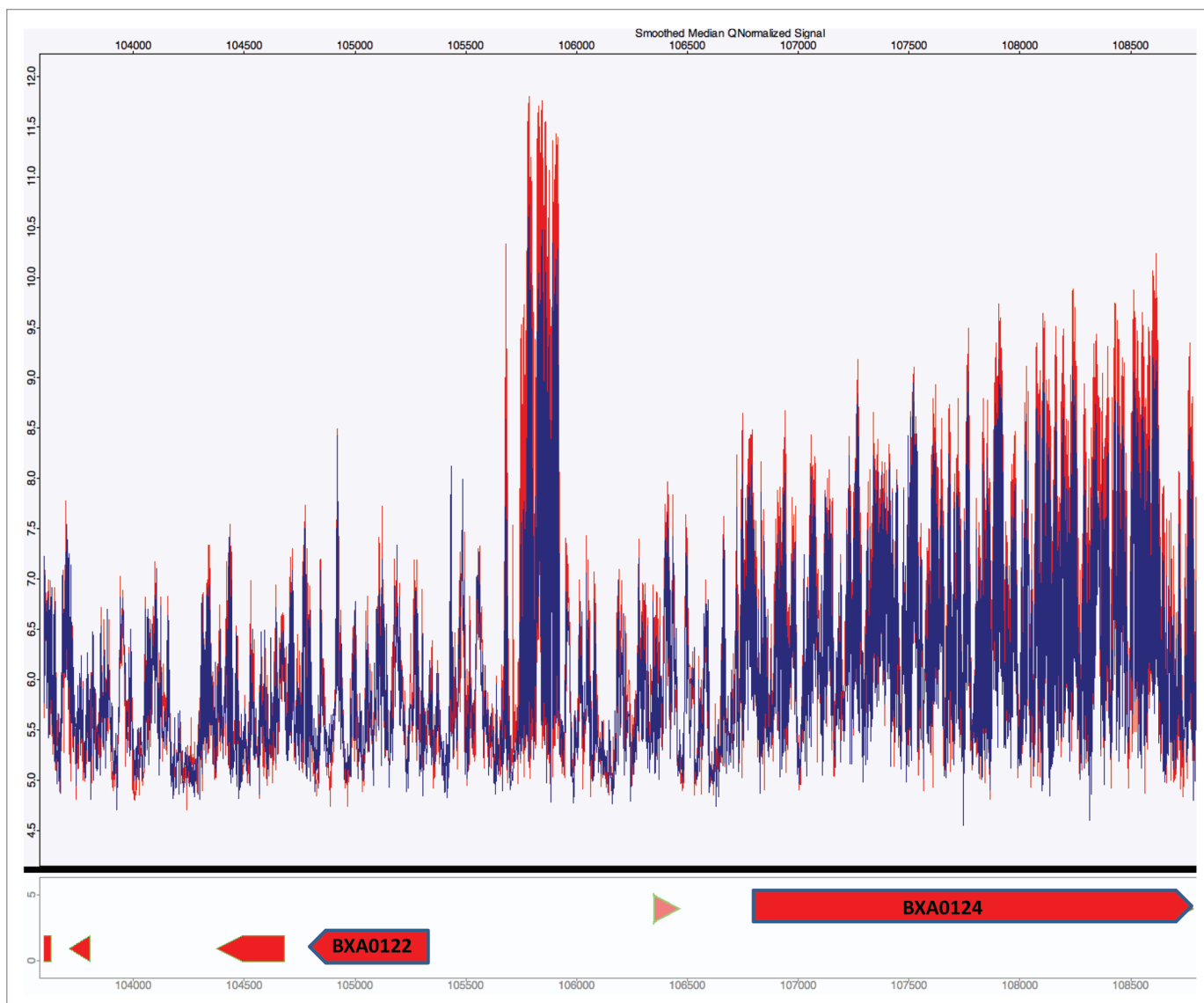


Figure 5. Analysis of small non-coding RNA of strain 34F₂Δ*luxS* compared to strain 34F₂ using an Affymetrix tiled array. A select region (between BXA0122 and BXA0124) based on pXOI from *B. anthracis* strain A2012, demonstrating transcriptional activity in intergenic regions. Red indicates the transcriptional activity of the parental strain and blue represents strain 34F₂Δ*luxS*.

has been observed in *Streptococcus pyogenes*.⁵⁰ In total, these data demonstrate that the altered phenotypes in the Δ*luxS* strain are due to *luxS* disruption and not to other undefined coincident mutations.

To better understand the role of *luxS*/AI-2-mediated QS in regulating *B. anthracis* gene expression and growth regulation, we utilized microarray analysis. Our use of microarrays permitted us to identify a number of genes potentially regulated by the *luxS*/AI-2 QS system, but which in total represent <1% of those in the *B. anthracis* genome. Downregulation in the Δ*luxS* strain of key virulence genes *pagA*, *pagR*, *lef* and *cya*, is notable. Inhibition of nitrate metabolism might explain the growth defect present in the 34F₂Δ*luxS* strain. The observed inhibition of the plasmid-encoded toxin gene expression may or may not be direct; AI-2 can modulate the expression of *Vibrio cholerae*

toxins in concert with small RNAs (sRNA).⁴⁴ Furthermore, recent data has demonstrated that small RNAs play a critical role in regulating virulence and sporulation in *V. cholerae* and *B. subtilis*, respectively.⁵¹⁻⁵⁴ One potential mechanism for *luxS*/AI-2-mediated quorum-sensing modulation of *B. anthracis* toxin expression is through the regulation of sRNAs. Detection of AI-2 by bacterial cells could potentially up or downmodulate regulatory small RNAs, leading to differential expression of the *B. anthracis* toxins.

To further understand the mechanisms by which *B. anthracis* utilizes the *luxS*/AI-2-mediated QS system to regulate growth-phase-dependent gene expression, we studied halogenated furanones, known inhibitors of QS.^{30-36,55} Furanone-1 [(5Z)-4-bromo-5-(bromomethylene)-3-butyl-2(5H)-furanone] has been shown to inhibit >70% of the AI-2 regulated genes in *E. coli*,

without affecting bacterial growth rate.³¹ We recently showed that halogenated furanones inhibit *B. anthracis* growth in a dose-dependent manner, and can inhibit the expression of *lacZ* when fused to the promoters of the toxin components.³⁰ The microarray analyses now reveal that treatment of cells with furanone (*fur-2*) results in inhibition of the transcription of virulence genes *lef* and *cya* on pXO1, and respiratory nitrate systems (Open reading frames BA2125-28, BA2133-38 and BA2142-46). Upstream sequence analysis of each potential operon revealed a conserved promoter motif, suggesting coordinate regulation of these operons (Suppl. Table 1). However this motif was not found upstream of *atxA* or other virulence genes. These data indicate that *fur-2* inhibits *B. anthracis* virulence gene expression and may lead to the development of a novel therapeutic agent against anthrax infections. In *Pseudomonas aeruginosa*, respiratory nitrate regulation has been implicated to be QS-dependent.⁵⁶

We conclude that *B. anthracis* utilizes *luxS* to regulate AI-2-dependent QS and bacterial growth; with specific regulation of expression of the S-layer protein EA1, respiratory nitrate systems and potentially, the lethal and edema toxins. We do recognize the limitation of our study working with an attenuated strain lacking pXO2. The experimentation performed in a pXO2-strain done for reasons concerning biosafety, however it would be fascinating to know what impact the pXO2-background might have on the gene expression patterns measure. We further conclude that the study of halogenated furanones may be used to guide development of novel inhibitors of *B. anthracis* virulence gene expression, as well as novel treatments for anthrax. Finally, identification of small RNAs on pXO1 suggests a novel mechanism for the regulation of virulence gene expression in *B. anthracis*. Further interrogating these small RNAs may illuminate greater understanding on how the toxins are expressed, since no *atxA* binding motif has ever been identified.

Materials and Methods

Bacterial strains and culture conditions. *B. anthracis* strains 34F₂ (Colorado Serum Company, Denver, CO), 34F₂Δ*luxS* and 34F₂Δ*luxS*:comp were routinely grown in Brain Heart Infusion broth (BHI) or BHI with 0.8% sodium bicarbonate at 37°C. *Escherichia coli* strain DH5α was routinely grown in Luria-Bertani broth (LB) at 37°C. Ampicillin (50 μg/ml) was added for cultivation of DH5α strains harboring recombinant plasmids. *V. harveyi* strain BB170, kindly provided by Bonnie Bassler (Princeton University, Princeton, NJ), was routinely grown in Auto-inducer Bioassay medium (AB) at 30°C.^{57,58}

Generation of cell-free culture medium and *V. harveyi* bioassays. *B. anthracis* strains were grown overnight with aeration at 37°C. Cell-free conditioned culture medium (CFM) was prepared by centrifugation of cultures at 4,000 rpm (Eppendorf Centrifuge 5810R) and passing the medium through a 0.2 μm pore-size MILLIPORE syringe filters (Carrigwohill Company, Cork, Ireland). CFM preparations were stored at -20°C until used. CFM from *V. harveyi* strain BB170 was prepared in the same manner, except that cultures were grown at 30°C. *V. harveyi*

Table 1. Oligonucleotide primers used in this study

Primer designation	Nucleotide sequence (5' → 3') ^a
PIF	TTTGAACGTGCGATGAAAG
P2R	GATTGTGGAAGCTGATGTAACAG
P3F	GCGGATCCATTGAAGAACTGCTGAAGCTC
P4R	GCGGATCCAGGAATAGATGTATATCAGAAC
P5F	CGTTAAAGCCTGATGTAAGCA
P6R	GGTTACGTGGTTGCTTAC
P9F	GCGGATCCTTAAAGTATTATAGCAGCACTG
PI0R	GCTCTACAATATCCAGTGTGCGAAACGTC
PI1F	GCGGTACCTTTGAACGTGCGATGAAAG
PI2R	GCGGTACCGATTGTGGAAGCTGATGTAACAG
BA <i>luxS</i> F	ATGCATCAGTAGAAAGCTTTG
BA <i>luxS</i> R	TTATCCAATACTTTCTCAAGTTC

^aRestriction sites underlined; *Bam*HI (GGATCC) and *Kpn*I (GGTACC).

bioluminescence assays were performed essentially as previously described.³⁷ Briefly, *V. harveyi* strain BB170 was grown at 30°C with aeration for 16 h, cultures were diluted 1:10,000 in fresh AB broth, and then 10% CFM or dilutions thereof from the bacterial cultures to be tested was added. Aliquots of 1.0-ml were taken 5 h after CFM was added, and bioluminescence measured, expressed as relative light units (RLU), using a luminometer.

Construction of a *B. anthracis* Δ*luxS*: complement strain. To complement the *luxS* deletion in *B. anthracis* strain 34F₂Δ*luxS*, the *plcR* operon, which encodes a pleiotropic regulator of hemolysins and phospholipases in *Bacillus cereus*, was selected as the site for integration of the *luxS* complementation cassette. In wild-type *B. anthracis* strains, *plcR* contains a nonsense mutation making it naturally inactive and thus a neutral spot for an in trans complementation locus.⁵⁹ The *luxS* ORF including its putative promoter were cloned into the *plcR* ORF. PCR was used to amplify a 3 kb fragment from the *plcR* locus, including 1.05 kb upstream and 1.1 kb downstream of the *plcR* ORF using primers P1 and P2 (Table 1). The PCR-amplified product was purified using a PCR purification kit (Qiagen, Valencia, CA), and subsequently cloned into pGEM-T easy. A plasmid with the correct insert and orientation was designated pMJ601. pMJ601 was modified by inverse PCR to add *Bam*HI sites (primers P3 and P4; Table 1) in the middle of the cloned insert for insertion of the *luxS* complementation cassette. The *luxS* complementation cassette was created by using purified chromosomal DNA of *B. anthracis* strain 34F₂. *B. anthracis luxS* was cloned using primers P9 and P10 to generate a 715-bp fragment including the putative *luxS* promoter. Downstream of the *luxS* ORF an erythromycin resistance cassette (Erm^R) was inserted into the *Xba*I/*Bam*HI site by restriction digest to enable selection for plasmid integration. Finally, primers P11 and P12 (Table 1) were used to clone the *plcR* region containing the *luxS*/Erm^R complementation cassette into *B. anthracis* shuttle vector pUTE29 that confers Tet^R. A plasmid with the correct insert was designated pMJ602ET. Purified pMJ602ET from SCS110 was electroporated into *B. anthracis* strain 34F₂:Δ*luxS* and colonies selected

Table 2. *B. anthracis* chromosomal genes upregulated in the 34F₂luxS strain as determined by microarray analysis, sorted by locus

Locus ^c	Gene Name ^b	30 min ^a	60 min	90 min	120 min
BA0194	oligopeptide ABC transporter, oligopeptide-binding protein	1.42	5.03	4.44	7.67
BA0369	methyl-accepting chemotaxis protein	6.15	11.47	6.68	6.28
BA0558	methyl-accepting chemotaxis protein	12.47	11.47	11.00	9.85
BA0575	methyl-accepting chemotaxis protein	4.86	7.16	6.45	8.51
BA0677	phospholipase C (plc)	4.14	7.06	5.28	6.54
BA0682	hypothetical protein	3.46	5.70	7.06	6.36
BA0796	conserved hypothetical protein	2.20	5.39	6.82	16.56
BA2025	hypothetical protein	9.32	14.22	10.85	12.73
BA2114	RNA polymerase sigma-70 factor, ECF subfamily	1.17	3.61	6.82	12.21
BA2115	hypothetical protein	1.68	3.48	7.84	9.99
BA2363	transcriptional regulator, ArsR family	3.78	11.63	12.38	7.67
BA2606	hypothetical protein	7.52	11.63	7.94	6.41
BA2732	RNA polymerase sigma factor SigX, putative	1.35	2.77	15.67	64.00
BA3029	succinylornithine transaminase, putative	1.23	4.89	7.41	7.78
BA3034	hypothetical protein	1.55	5.06	4.23	8.22
BA3114	membrane protein, putative	13.45	10.78	7.36	11.24
BA3305	transcriptional regulator, ArsR family	3.76	7.67	5.06	10.34
BA3405	ABC transporter, permease protein	1.28	1.83	8.57	11.63
BA3406	ABC transporter, ATP-binding protein	0.71	2.46	6.77	18.13
BA3407	hypothetical protein	1.08	2.22	7.11	8.28
BA4264	nitroreductase family protein	1.52	2.81	3.97	7.16
BA5481	conserved domain protein	7.31	14.03	4.89	7.26
BA5628	iron compound ABC transporter	1.85	4.11	3.76	7.01

^aNumbers represent fold change over the 120 min time course of the experiments; ^bFunctional annotations were obtained from the *B. anthracis* complete genome sequence (www.jcvi.org); ^cLocus based on Ames strain of *B. anthracis*.

for erythromycin resistance. Transformants were initially picked on medium containing 5 µg/ml of erythromycin, and then subcultured twice daily in the absence of antibiotics at 37° with aeration, for 15 days. Individual colonies were subsequently screened to identify clones that were both Erm^R and Tet^S. This would suggest loss of pMJ602ET and incorporation of the modified *plcR* allele into the chromosome. For clones with the appropriate antibiotic phenotype, the correct insertion was confirmed by PCR using primers luxSF/P6 and luxSR/P5 (Table 1).

RNA isolation for microarray analysis. *B. anthracis* RNA was isolated from bacterial cultures grown to mid-log in BHI media with or without sodium bicarbonate, RNAProtect (Qiagen) was directly added to the growth media at a concentration of 2:1 (volume of RNAProtect to bacterial culture). RNA was isolated from bacterial cultures grown in the presence of or the absence of furanone-2 (fur-2; 3-butyl-5-(dibromomethylene)-2-(5H)-furanone), as stated above. Cells treated with RNAProtect were pelleted and stored at -80°C until RNA extraction, using the Ambion mirVana RNA kit (Austin, TX) in combination with the Barocycler (Pressure BioSciences, South Easton, MA). RNA quantity and quality was assessed by measuring total RNA using a nanodrop 1000 spectrophotometer (Thermo Scientific) and visualizing RNA on an agarose gel. Purified RNA was stored at -80°C.

Generation of probes for microarray experiments. DNA probes for microarray experiments were generated by adding 2 µg of total RNA in a mixture containing 6 µg of random hexamers (Invitrogen), 0.01 M dithiothreitol, an aminoallyl-deoxynucleoside triphosphate mixture containing 25 mM each dATP, dCTP and dGTP, 15 mM dTTP, and 10 mM amino-allyl-dUTP (aa-dUTP) (Sigma), reaction buffer, and 400 units of SuperScript III reverse transcriptase (Invitrogen) at 42°C overnight. The RNA template then was hydrolyzed by adding NaOH and EDTA to a final concentration of 0.2 and 0.1 M, respectively, and incubating at 65°C for 15 min. Unincorporated aa-dUTP was removed with a Minelute column (Qiagen). The probe was eluted with a phosphate elution buffer (4 mM KPO₄, pH 8.5, in ultrapure water), dried and resuspended in 0.1 M sodium carbonate buffer (pH 9.0). To couple the amino-allyl cDNA with fluorescent labels, normal human serum-Cy3 or normal human serum-Cy5 (Amersham) was added at room temperature for 1 h. Uncoupled label was removed using the Qiagen Minelute column (Valencia, CA) (intranet.jtc.jcvf.org/sops/M007.pdf).

Microarray hybridization, scanning, image analysis, normalization and analysis. Aminosilane-coated slides printed with a set of 15,552 *B. anthracis* open reading frame sequences (www.jcvi.org) were prehybridized in 5x SSC (1x SSC is 0.15 M NaCl plus 0.015 M sodium citrate) (Invitrogen), 0.1% sodium dodecyl

Table 3. *B. anthracis* chromosomal genes downregulated in the 34F₂Δ*luxS* strain as determined by microarray analysis, sorted by locus

Locus ^c	Gene name ^b	30 min ^a	60 min	90 min	120 min
BA0238	hypothetical protein	-3.41	-29.65	-5.78	-15.78
BA0239	hypothetical protein	-3.86	-22.16	-5.86	-19.29
BA0240	4-hydroxyphenylpyruvate dioxygenase (<i>hppD</i>)	NaN	-11.63	-9.51	-6.41
BA0509	formate acetyltransferase (<i>pfl</i>)	-33.13	-125.37	-56.89	-35.51
BA0510	pyruvate formate-lyase-activating enzyme (<i>pflA</i>)	-1.26	-23.26	-36.00	-21.71
BA0668	ribose ABC transporter, permease protein (<i>rbsC</i>)	-1.42	-14.42	-12.91	-7.94
BA0669	ribose ABC transporter, ribose-binding protein (<i>rbsB</i>)	-1.58	-15.89	-11.88	-6.96
BA0887	S-layer protein EAI (<i>eag</i>)	-7.26	-25.63	-46.85	-3.97
BA1086	sugar-binding transcriptional regulator, LacI family	-3.14	-19.29	-11.08	-4.20
BA2125	respiratory nitrate reductase, alpha subunit (<i>narG</i>)	-6.68	-4.20	-52.71	-42.22
BA2126	respiratory nitrate reductase, beta subunit (<i>narH</i>)	-1.13	-3.18	-29.24	-17.39
BA2128	respiratory nitrate reductase, gamma subunit (<i>narI</i>)	-1.25	-3.12	-38.59	-18.13
BA2133	molybdenum cofactor biosynthesis protein A (<i>narA-I</i>)	-1.84	-6.36	-45.25	-14.83
BA2134	molybdopterin biosynthesis protein MoeB, putative	-1.07	-5.06	-103.97	-13.55
BA2135	molybdopterin biosynthesis protein MoeA (<i>moeA-I</i>)	-1.12	-2.19	-35.26	-13.64
BA2136	molybdopterin converting factor, subunit 2 (<i>moaE-I</i>)	-1.13	-2.95	-48.84	-20.53
BA2137	molybdopterin converting factor, subunit 1 (<i>moaD-I</i>)	-1.36	-1.91	-22.78	-29.86
BA2138	nitrate transporter (<i>narK</i>)	-1.24	-1.92	-37.53	-21.11
BA2146	nitrite reductase [NAD(P)H], large subunit (<i>nirB</i>)	-1.33	-76.11	-60.97	-210.84
BA2267	alcohol dehydrogenase, zinc-containing	-3.61	-12.91	-6.45	-9.19
BA2295	acetate CoA-transferase, subunit A (<i>atoD</i>)	-1.01	NaN	-8.11	-22.16
BA2350	carboxyvinyl-carboxyphosphonate phosphorylmutase (<i>yqiQ</i>)	-1.52	-5.24	-12.13	-19.16
BA2547	acyl-CoA dehydrogenase	-2.01	-13.36	-19.70	-10.48
BA2548	acetyl-CoA carboxylase, biotin carboxylase, putative	-1.66	-7.06	-17.27	-9.99
BA2552	carboxyl transferase domain protein	-1.24	-16.45	-11.39	-10.27
BA3479	transcriptional regulator, ArsR family	-36.00	-44.94	-37.27	-136.24
BA3481	hypothetical protein	-38.85	-315.17	-137.19	-69.55
BA3482	conserved hypothetical protein	-32.67	-36.00	-64.45	-140.07
BA3483	conserved hypothetical protein	-30.48	-67.18	-53.82	-219.79
BA3663	anaerobic ribonucleoside-triphosphate reductase	NaN	-14.03	-4.66	-9.92
BA5047	autoinducer-2 production protein LuxS (<i>luxS</i>)	-14.72	-28.84	-29.86	-494.56
BA5696	superoxide dismutase, Mn (<i>sodA-2</i>)	-1.77	-7.62	-14.62	-7.11

^aNumbers represent fold change over the 120 min time course of the experiments; ^bFunctional annotations were obtained from the *B. anthracis* complete genome sequence (www.jcvi.org); ^cLocus based on Ames strain of *B. anthracis*; ^dNaN indicates a miss data point.

sulfate and 1% bovine serum albumin at 42°C for 60 min. The slides then were washed at room temperature with distilled water, dipped in isopropanol and allowed to dry. Equal volumes of the appropriate Cy3- and Cy5-labeled probes were combined, dried and then resuspended in a solution of 40% formamide, 5x SSC and 0.1% sodium dodecyl sulfate. Resuspended probes were heated to 95°C prior to hybridization. The probe mixture then was added to the microarray slide and allowed to hybridize overnight at 42°C. Hybridized slides were washed sequentially in solutions of 1x SSC-0.2% SDS, 0.1x SSC-0.2% SDS and 0.1x SSC at room temperature, then dried in air and scanned with an Axon GenePix 4000 scanner (intranet.jtc.jcvf.org/sops/M008.pdf). All wash buffers were supplemented with 1-ml of 0.1 M DTT per liter of wash buffer. Individual TIFF images from each

channel were analyzed with TIGR Spotfinder (available at (pfgrc.jcvi.org/index.php/bioinformatics.html)). Microarray data were normalized by LOWESS normalization and with in-slide replicate analysis using TM4 software MIDAS (available at (pfgrc.jcvi.org/index.php/bioinformatics.html)).^{38,60} We selected genes in which comparison of wild-type cells exposed to diluent alone and cells exposed to 20 µg/ml of fur-2 yielded log₂ value |≥1.5| in all samples. We also selected genes that had a log₂ value |≥1.5| in all samples, comparing wild-type cells to Δ*luxS* cells. Genes with a log₂ value |≤1.5| but a log₂ value |≥1| were selected if the gene appeared in the middle of an operon.

Analysis of upstream promoter motifs. A selected set of genes that appeared to be co-regulated in the linear expression map were analyzed to discover motifs in upstream areas that may identify

Table 4. Select genes downregulated on pXOI in *B. anthracis* 34F₂Δ*luxS* as determined by microarray analysis, sorted by locus

Locus ^c	Gene name ^b	30 min ^a	60 min	90 min	120 min
BXA0142	calmodulin-sensitive adenylate cyclase (<i>cya</i>)	1.03	-2.00	-3.46	-4.69
BXA0146	transcriptional activator <i>AtxA</i> (<i>atxA</i>)	-1.34	-1.16	-1.25	-1.83
BXA0164	protective antigen (<i>pagA</i>)	-1.02	-1.53	-7.21	-26.17
BXA0165	hypothetical protein	1.21	-1.74	-7.52	-20.97
BXA0166	transcriptional repressor <i>PagR</i> (<i>pagR</i>)	-1.13	-2.13	-6.11	-13.36
BXA0167	hypothetical protein	1.36	-1.39	-5.70	-10.27
BXA0168	hypothetical protein	-1.20	-1.13	-2.46	-2.62
BXA0169	hypothetical protein	-1.23	-1.20	-2.10	-2.89
BXA0170	hypothetical protein	-1.24	1.16	-1.71	-4.23
BXA0171	ribonuclease domain protein	-1.59	-1.49	-2.99	-7.62
BXA0172	lethal factor (<i>lef</i>)	-1.02	1.05	-2.71	-4.92

^aNumbers represent fold change over the 120 min time course of the experiments; Bolded genes indicate genes involved in *B. anthracis* toxin production or its regulation; ^bFunctional annotations were obtained from the *B. anthracis* complete genome sequence (www.jcvi.org); ^cLocus based on Ames strain of *B. anthracis*.

Table 5. Select virulence genes downregulated on pXOI in 34F₂Δ*luxS* compared to 34F₂*luxS*:comp

Locus ^c	Gene name ^b	120 min ^a
BXA0124	S-layer protein	-5.16
BXA0142	calmodulin-sensitive adenylate cyclase	-3.97
BXA0146	transcriptional activator <i>AtxA</i>	-2.9
BXA0164	protective antigen	-13.78
BXA0165	hypothetical protein	-16.83
BXA0166	transcriptional repressor <i>PagR</i>	-14.66
BXA0172	lethal factor	-4.32

^aNumbers represent fold change over; Bolded genes indicate genes involved in *B. anthracis* toxin production or its regulation; ^bFunctional annotations were obtained from the *B. anthracis* complete genome sequence (www.jcvi.org); ^cLocus based on *B. anthracis* strain A2012.

Table 6. Select *B. anthracis* genes on pXOI downregulated by *fur-2*

Locus ^c	Gene name ^b	Symbol	120 min ^a
BXA0124	S-layer protein		-16.63
BXA0142	calmodulin-sensitive adenylate cyclase	<i>cyaA</i>	-1.41
BXA0146	transcriptional activator <i>AtxA</i>	<i>atxA</i>	-1.34
BXA0164	protective antigen	<i>pagA</i>	-13.48
BXA0166	transcriptional repressor <i>PagR</i>	<i>pagR</i>	-5.81
BXA0172	lethal factor	<i>lef</i>	-2.03

^aNumbers represent fold change; ^bFunctional annotations were obtained from the *B. anthracis* complete genome sequence (www.jcvi.org); ^cLocus based on *B. anthracis* strain A2012.

common transcription factor binding sites. For motif discovery analysis, 200 base sequences upstream of each gene in the genome were collected. These upstream sequences were truncated when necessary to exclude sequences that crossed a neighboring gene boundary. Upstream sequences less than 30 bases were excluded. If the gene was transcribed on the minus strand, the reverse complement of the upstream region was analyzed. Motif finding was performed using

the discriminative motif finding tool, DEME.⁶¹ DEME requires two input sequence lists; one input corresponds to upstream areas believed to possibly contain a shared motif and the other set consists of upstream sequences of genes that are thought to not contain the motif within the positive group. The algorithm attempts to find a motif that best separates the positive group of upstream sequences corresponding to the co-regulated gene

set from the negative set, representing all other upstream sequences in the genome. A 15 base window was used and the reverse complement of each upstream section also was analyzed. DEME reports a consensus motif and upstream sequence matches for each positive *and* negative sequence. NCBI refseq was the source for the whole genome sequence file and the coordinate file (ptt file) used to extract upstream sequences.

Analysis of small RNAs in *B. anthracis* 34F₂Δ*luxS* strain. Cells were grown to early log phase and pellets collected at 30, 60, 90 and 120 minutes. Total RNA was extracted from cell pellets previously treated with RNAProtect (Qiagen), and the extracted RNAs were treated with Turbo DNA-free DNase (Ambion), then converted to cDNA and labeled according to the Affymetrix protocol. Labeled probes were hybridized onto the Affymetrix platform and incubated overnight in an Affymetrix oven. Chips were washed, scanned and .CEL files were imported into genomeMTV (www.genomeMTV.org) for analysis. Data were normalized by the genomeMTV software, based on quantum normalization. Analysis of pXO1 using the sliding window of genomeMTV

permitted us to visually scan the virulence plasmid and inspect for intergenic transcriptional activity.

Acknowledgements

We thank Michael Garabedian for providing instrumentation. This work was supported in part by the Medical Research Service of the Department of Veterans Affairs, the Northeast Biodefense Center NIAID Regional Center for Excellence (U54 AI057158), ROI AI 068409 from the National Institutes of Health, the American Association for the Advancement of Science (AAAS), David and Lucile Packard Foundation, the UNCF/Merck Graduate Dissertation Fellowship, the Pathogen Functional Genomics Resource Center (PFGR) contract (contract No. N01-AI15447) and funding by the National Institute of Allergy and Infectious Diseases of the National Institutes of Health.

Note

Supplementary materials can be found at:

www.landesbioscience.com/supplement/JonesVIRUI-2-Sup1.xls

www.landesbioscience.com/supplement/JonesVIRUI-2-Sup2.pdf

References

- Dutz W, Kohout E. Anthrax. *Pathol Annu* 1971; 6:209-48.
- Hambleton P, Carman JA, Melling J. Anthrax: the disease in relation to vaccines. *Vaccine* 1984; 2:125-32.
- Turnbull PC. Anthrax vaccines: past, present and future. *Vaccine* 1991; 9:533-9.
- Ullmann A, Mock M. A particular class of virulence factors: calmodulin-activated bacterial adenylate cyclases. *Zentralbl Bakteriol* 1994; 281:284-95.
- Makino S, Uchida I. The pathogenesis of *Bacillus anthracis*. *Nippon Saikingu Zasshi* 1996; 51:833-40.
- Hanna PC, Ireland JA. Understanding *Bacillus anthracis* pathogenesis. *Trends Microbiol* 1999; 7:180-2.
- Brossier F, Mock M. Toxins of *Bacillus anthracis*. *Toxicon* 2001; 39:1747-55.
- Mock M, Fouet A. Anthrax. *Annu Rev Microbiol* 2001; 55:647-71.
- Koehler TM. *Bacillus anthracis* genetics and virulence gene regulation. *Curr Top Microbiol Immunol* 2002; 271:143-64.
- Mock M, Mignot T. Anthrax toxins and the host: a story of intimacy. *Cell Microbiol* 2003; 5:15-23.
- Ahuja N, Kumar P, Bhatnagar R. The adenylate cyclase toxins. *Crit Rev Microbiol* 2004; 30:187-96.
- Moayeri M, Leppla SH. The roles of anthrax toxin in pathogenesis. *Curr Opin Microbiol* 2004; 7:19-24.
- Mock M, Ullmann A. Calmodulin-activated bacterial adenylate cyclases as virulence factors. *Trends Microbiol* 1993; 1:187-92.
- Brossier F, Guidi-Rontani C, Mock M. Anthrax toxins. *C R Seances Soc Biol Fil* 1998; 192:437-44.
- Hanna P. Anthrax pathogenesis and host response. *Curr Top Microbiol Immunol* 1998; 225:13-35.
- Little SF, Ivins BE. Molecular pathogenesis of *Bacillus anthracis* infection. *Microbes Infect* 1999; 1:131-9.
- Liu S, Schubert RL, Bugge TH, Leppla SH. Anthrax toxin: structures, functions and tumour targeting. *Expert Opin Biol Ther* 2003; 3:843-53.
- Abrami L, Reig N, van der Goot FG. Anthrax toxin: the long and winding road that leads to the kill. *Trends Microbiol* 2005; 13:72-8.
- Sirard JC, Mock M, Fouet A. The three *Bacillus anthracis* toxin genes are coordinately regulated by bicarbonate and temperature. *J Bacteriol* 1994; 176:5188-92.
- Gray KM. Intercellular communication and group behavior in bacteria. *Trends Microbiol* 1997; 5:184-8.
- Morrison DA. Streptococcal competence for genetic transformation: regulation by peptide pheromones. *Microb Drug Resist* 1997; 3:27-37.
- Hardman AM, Stewart GS, Williams P. Quorum sensing and the cell-cell communication dependent regulation of gene expression in pathogenic and non-pathogenic bacteria. *Antonie Van Leeuwenhoek* 1998; 74:199-210.
- Bassler BL. How bacteria talk to each other: regulation of gene expression by quorum sensing. *Curr Opin Microbiol* 1999; 2:582-7.
- Miller MB, Bassler BL. Quorum sensing in bacteria. *Annu Rev Microbiol* 2001; 55:165-99.
- Bassler BL. Small talk. Cell-to-cell communication in bacteria. *Cell* 2002; 109:421-4.
- Manefield M, Welch M, Givskov M, Salmond GP, Kjelleberg S. Halogenated furanones from the red alga, *Delisea pulchra*, inhibit carbapenem antibiotic synthesis and exoenzyme virulence factor production in the phytopathogen *Erwinia carotovora*. *FEMS Microbiol Lett* 2001; 205:131-8.
- Hentzer M, Givskov M. Pharmacological inhibition of quorum sensing for the treatment of chronic bacterial infections. *J Clin Invest* 2003; 112:1300-7.
- Hentzer M, Wu H, Andersen JB, Riedel K, Rasmussen TB, Bagge N, et al. Attenuation of *Pseudomonas aeruginosa* virulence by quorum sensing inhibitors. *EMBO J* 2003; 22:3803-15.
- Smith KM, Bu Y, Suga H. Induction and inhibition of *Pseudomonas aeruginosa* quorum sensing by synthetic autoinducer analogs. *Chem Biol* 2003; 10:81-9.
- Jones MB, Jani R, Ren D, Wood TK, Blaser MJ. Inhibition of *Bacillus anthracis* Growth and Virulence- Gene Expression by Inhibitors of Quorum-Sensing. *J Infect Dis* 2005; 191:1881-8.
- Ren D, Bedzyk LA, Ye RW, Thomas SM, Wood TK. Differential gene expression shows natural brominated furanones interfere with the autoinducer-2 bacterial signaling system of *Escherichia coli*. *Biotechnol Bioeng* 2004; 88:630-42.
- Ren D, Bedzyk LA, Setlow P, England DF, Kjelleberg S, Thomas SM, et al. Differential gene expression to investigate the effect of (5Z)-4-bromo-5-(bromomethylene)-3-butyl-2(5H)-furanone on *Bacillus subtilis*. *Appl Environ Microbiol* 2004; 70:4941-9.
- Ren D, Zuo R, Wood TK. Quorum-sensing antagonist (5Z)-4-bromo-5-(bromomethylene)-3-butyl-2(5H)-furanone influences siderophore biosynthesis in *Pseudomonas putida* and *Pseudomonas aeruginosa*. *Appl Microbiol Biotechnol* 2005; 66:689-95.
- Ren D, Wood TK. (5Z)-4-bromo-5-(bromomethylene)-3-butyl-2(5H)-furanone reduces corrosion from *Desulfotomaculum orientis*. *Environ Microbiol* 2004; 6:535-40.
- Ren D, Sims JJ, Wood TK. Inhibition of biofilm formation and swarming of *Bacillus subtilis* by (5Z)-4-bromo-5-(bromomethylene)-3-butyl-2(5H)-furanone. *Lett Appl Microbiol* 2002; 34:293-9.
- Ren D, Sims JJ, Wood TK. Inhibition of biofilm formation and swarming of *Escherichia coli* by (5Z)-4-bromo-5-(bromomethylene)-3-butyl-2(5H)-furanone. *Environ Microbiol* 2001; 3:731-6.
- Jones MB, Blaser MJ. Detection of a luxS-signaling molecule in *Bacillus anthracis*. *Infect Immun* 2003; 71:3914-9.
- Saeed AI, Sharov V, White J, Li J, Liang W, Bhagabati N, et al. TM4: a free, open-source system for microarray data management and analysis. *Biotechniques* 2003; 34:374-8.
- Morozkina EV, Zvyagilskaya RA. Nitrate reductases: structure, functions and effect of stress factors. *Biochemistry (Mosc)* 2007; 72:1151-60.
- Nakano MM, Yang F, Hardin P, Zuber P. Nitrogen regulation of nasA and the nasB operon, which encode genes required for nitrate assimilation in *Bacillus subtilis*. *J Bacteriol* 1995; 177:573-9.
- Ahmer BM, van Reeuwijk J, Timmers CD, Valentine PJ, Heffron F. *Salmonella typhimurium* encodes an SdiA homolog, a putative quorum sensor of the LuxR family, that regulates genes on the virulence plasmid. *J Bacteriol* 1998; 180:1185-93.
- Manefield M, Harris L, Rice SA, de Nys R, Kjelleberg S. Inhibition of luminescence and virulence in the black tiger prawn (*Penaeus monodon*) pathogen *Vibrio harveyi* by intercellular signal antagonists. *Appl Environ Microbiol* 2000; 66:2079-84.
- Hentzer M, Riedel K, Rasmussen TB, Heydorn A, Andersen JB, Parsek MR, et al. Inhibition of quorum sensing in *Pseudomonas aeruginosa* biofilm bacteria by a halogenated furanone compound. *Microbiology* 2002; 148:87-102.

44. Miller MB, Skorupski K, Lenz DH, Taylor RK, Bassler BL. Parallel quorum sensing systems converge to regulate virulence in *Vibrio cholerae*. *Cell* 2002; 110:303-14.
45. Whitehead NA, Byers JT, Commander P, Corbett MJ, Coulthurst SJ, Everson L, et al. The regulation of virulence in phytopathogenic *Erwinia* species: quorum sensing, antibiotics and ecological considerations. *Antonie Van Leeuwenhoek* 2002; 81:223-31.
46. Haralalka S, Nandi S, Bhadra RK. Mutation in the *relA* gene of *Vibrio cholerae* affects in vitro and in vivo expression of virulence factors. *J Bacteriol* 2003; 185:4672-82.
47. Manna AC, Cheung AL. *sarU*, a *sarA* homolog, is repressed by *SarT* and regulates virulence genes in *Staphylococcus aureus*. *Infect Immun* 2003; 71:343-53.
48. Novick RP, Jiang D. The staphylococcal *saeRS* system coordinates environmental signals with *agr* quorum sensing. *Microbiology* 2003; 149:2709-17.
49. Hammer BK, Bassler BL. Quorum sensing controls biofilm formation in *Vibrio cholerae*. *Mol Microbiol* 2003; 50:101-4.
50. Lyon WR, Madden JC, Levin JC, Stein JL, Caparon MG. Mutation of *luxS* affects growth and virulence factor expression in *Streptococcus pyogenes*. *Mol Microbiol* 2001; 42:145-57.
51. Lenz DH, Bassler BL. The small nucleoid protein *Fis* is involved in *Vibrio cholerae* quorum sensing. *Mol Microbiol* 2007; 63:859-71.
52. Lenz DH, Miller MB, Zhu J, Kulkarni RV, Bassler BL. *CsrA* and three redundant small RNAs regulate quorum sensing in *Vibrio cholerae*. *Mol Microbiol* 2005; 58:1186-202.
53. Lenz DH, Mok KC, Lilley BN, Kulkarni RV, Wingreen NS, Bassler BL. The small RNA chaperone *Hfq* and multiple small RNAs control quorum sensing in *Vibrio harveyi* and *Vibrio cholerae*. *Cell* 2004; 118:69-82.
54. Ding Y, Davis BM, Waldor MK. *Hfq* is essential for *Vibrio cholerae* virulence and downregulates sigma expression. *Mol Microbiol* 2004; 53:345-54.
55. Ren D, Zuo R, Wood TK. Quorum-sensing antagonist (5Z)-4-bromo-5-(bromomethylene)-3-butyl-2(5H)-furanone influences siderophore biosynthesis in *Pseudomonas putida* and *Pseudomonas aeruginosa*. *Appl Microbiol Biotechnol* 2004.
56. Toyofuku M, Nomura N, Kuno E, Tashiro Y, Nakajima T, Uchiyama H. Influence of the *Pseudomonas quinolone* signal on denitrification in *Pseudomonas aeruginosa*. *J Bacteriol* 2008; 190:7947-56.
57. Bassler BL, Greenberg EP, Stevens AM. Cross-species induction of luminescence in the quorum-sensing bacterium *Vibrio harveyi*. *J Bacteriol* 1997; 179:4043-5.
58. Bassler BL, Wright M, Silverman MR. Multiple signaling systems controlling expression of luminescence in *Vibrio harveyi*: sequence and function of genes encoding a second sensory pathway. *Mol Microbiol* 1994; 13:273-86.
59. Agaisse H, Gominet M, Okstad OA, Kolsto AB, Lereclus D. *PlcR* is a pleiotropic regulator of extracellular virulence factor gene expression in *Bacillus thuringiensis*. *Mol Microbiol* 1999; 32:1043-53.
60. Saeed AI, Bhagabati NK, Braisted JC, Liang W, Sharov V, Howe EA, et al. TM4 microarray software suite. *Methods Enzymol* 2006; 411:134-93.
61. Redhead E, Bailey TL. Discriminative motif discovery in DNA and protein sequences using the DEME algorithm. *BMC Bioinformatics* 2007; 8:385.